Published February 18, 2013

JEM

Endothelial cell–specific lymphotoxin-β receptor signaling is critical for lymph node and high endothelial venule formation

Lucas Onder,[1] Renzo Danuser,[2] Elke Scandella,[1] Sonja Firner,[1] Qian Chai,[1] Thomas Hehlgans,[3] Jens V. Stein,[2] and Burkhard Ludewig[1]

[1]Institute of Immunobiology, Kantonal Hospital St. Gallen, CH-9007 St. Gallen, Switzerland
[2]Theodor Kocher Institute, University of Bern, CH-3012 Bern, Switzerland
[3]Institute of Immunology, University of Regensburg, 93053 Regensburg, Germany

The development of lymph nodes (LNs) and formation of LN stromal cell microenvironments is dependent on lymphotoxin-β receptor (LTβR) signaling. In particular, the LTβR-dependent crosstalk between mesenchymal lymphoid tissue organizer and hematopoietic lymphoid tissue inducer cells has been regarded as critical for these processes. Here, we assessed whether endothelial cell (EC)–restricted LTβR signaling impacts on LN development and the vascular LN microenvironment. Using EC-specific ablation of LTβR in mice, we found that conditionally LTβR-deficient animals failed to develop a significant proportion of their peripheral LNs. However, remnant LNs showed impaired formation of high endothelial venules (HEVs). Venules had lost their cuboidal shape, showed reduced segment length and branching points, and reduced adhesion molecule and constitutive chemokine expression. Due to the altered EC–lymphocyte interaction, homing of lymphocytes to peripheral LNs was significantly impaired. Thus, this study identifies ECs as an important LTβR-dependent lymphoid tissue organizer cell population and indicates that continuous triggering of the LTβR on LN ECs is critical for lymphocyte homeostasis.

CORRESPONDENCE
Burkhard Ludewig:
burkhard.ludewig@kssg.ch

Abbreviations used: EC, endothelial cell; FRC, fibroblastic reticular cell; HEV, high endothelial venule; ICAM-1, intercellular adhesion molecule 1; LEC, lymphatic EC; LTβR, lymphotoxin-β receptor; LTi, lymphoid tissue inducer; LTo, lymphoid tissue organizer; OPT, optical projection tomographical; VE-cadherin, vascular endothelial cadherin.

LNs concentrate hematopoietic cells and pathogens at distinct sites of the mammalian anatomy to facilitate optimal induction of protective immune responses (Junt et al., 2008). The structural organization of LNs is determined by different stromal cells that form specific microenvironments for lymphocyte entry and exit and the optimized interaction between different leukocyte populations (Turley et al., 2010). The development of LNs is a well-orchestrated process that is thought to mainly involve the lymphotoxin-β receptor (LTβR)–dependent crosstalk between mesenchymal lymphoid tissue organizer (LTo) and hematopoietic lymphoid tissue inducer (LTi) cells (van de Pavert and Mebius, 2010). Indeed, LTβR-dependent stromal organizer cells can be demonstrated in developing LNs, which most likely give rise to mesenchymal stromal cell subpopulations in adult LNs (Bénézech et al., 2010). However, the developmental relationship of stromal cell sublineages has only recently been investigated (Malhotra et al., 2012), and hence the genuine contribution of different stromal cells to LN development has remained poorly understood. In fact, endothelial cells (ECs) are among the first participants in the formation of the LN anlage (Blum and Pabst, 2006). In mice, endothelial progenitors leave the cardinal vein at embryonic day 9 and form the lymph sac, the primordial tissue of the lymphatic system (Oliver and Srinivasan, 2008). Only later do mesenchymal LTo and hematopoietic LTi cells establish their interaction and foster LN growth (Blum and Pabst, 2006). Hence, we considered it possible that ECs participate in LN development and that LTβR signals may impact on the developing LN vasculature.

Lymphocytes enter and exit the LN parenchyma either through lymphatic endothelia in the LN medulla (Braun et al., 2011) or via high endothelial venules (HEVs) in the interfollicular regions (Grigorova et al., 2010). High endothelial cells exhibit a cuboidal shape and a polarized

The Rockefeller University Press $30.00
J. Exp. Med. 2013 Vol. 210 No. 3 465-473
www.jem.org/cgi/doi/10.1084/jem.20121462

Published February 18, 2013

organization with luminal localization of adhesion molecules such as intercellular adhesion molecule 1 (ICAM-1), which functions as anchors for cells circulating in the blood (Tohya et al., 2010). LTβR signals are important for the maintenance the HEV network under homeostatic conditions, as demonstrated by systemic treatment of adult mice with an LTβR decoy receptor (Browning et al., 2005). Furthermore, myeloid lymphotoxin-expressing cells, such as dendritic cells, can interact with HEV ECs to stimulate their maturation (Moussion and Girard, 2011). However, other LN stromal cells, including fibroblastic reticular cells (FRCs), can be efficiently triggered via the LTβR to secrete potent vascular growth factors, establishing a multicellular regulation circuit that maintains the homeostasis of the HEV network (Chyou et al., 2008). Thus, it has remained elusive whether the generation and maintenance of HEV morphology and function is determined by direct LTβR signals in ECs or whether LTβR-dependent communication between different LN stromal cell populations generates the appropriate microenvironment.

To assess the impact of specific and constitutive ablation of LTβR signaling in ECs, we crossed vascular endothelial cadherin (VE-cadherin)-Cre mice (Alva et al., 2006) with *Ltβr*$^{fl/fl}$ mice (Wimmer et al., 2012). We found that the specific deletion of the LTβR on ECs blocked the development of a significant proportion of peripheral LNs. Furthermore, EC-specific LTβR signaling was critical for formation of the HEV network and control of lymphocyte trafficking.

RESULTS AND DISCUSSION

Targeting of LTβR-expressing ECs with the *VE-cadherin-Cre* transgene

LTβR is broadly expressed in various tissues of the developing mouse embryo (Browning and French, 2002), and LTβR deficiency severely impairs the development of peripheral lymphoid tissues (Fütterer et al., 1998). To assess the LTβR expression pattern in major LN stromal cell populations, we separated CD45$^-$ stromal cells by FACS sorting using the well-established markers podoplanin and CD31 (Malhotra et al., 2012) into Pdpn$^-$CD31$^+$ blood ECs (BECs), Pdpn$^+$CD31$^+$ lymphatic ECs (LECs), and Pdpn$^-$CD31$^+$ FRCs (Fig. 1 a). Mesenchymal versus endothelial lineage identity of the sorted cell populations was confirmed by exclusive *Wnt1* mRNA expression in the FRC fraction (Fig. 1 b). *Ltβr* mRNA expression was comparable in the three major LN stromal cell populations (Fig. 1 c), whereas LTβR expression on the surface of both BECs and LECs was significantly higher compared with FRCs (Fig. 1, d and e) suggesting that ligation of the LTβR on ECs may precipitate important functional changes in ECs.

To assess the developmental and functional consequences of LTβR ablation in ECs, we used transgenic *VE-cadherin-Cre* mice. In these mice, *VE-Cadherin-Cre* activity starts in the embryonic endothelium at E8, i.e., before the initial steps of LN development (Alva et al., 2006). At E16.5, transgene-expressing ECs co-localized with CD4$^+$ LTi cells in the anlage of the inguinal LN (Fig. 2 a). Importantly, transgene activity in developing inguinal LNs (E18.5) of *VE-Cadherin-CrexR26-RFP* mice was not associated with CD45$^+$ cells (Fig. 2 b). Likewise, in neonatal LNs, transgene expression was confined to CD31$^+$ ECs (Fig. 2 c). Importantly, ECs in the neonatal LN coexpressed LTβR and the *VE-cadherin-Cre* transgene, with the highest abundance in the region of the subcapsular sinus (Fig. 2 c, i–iv). Confocal microscopic (Fig. 2 d) and flow cytometric (Fig. 2 e) analysis of adult LNs from *VE-cadherin-CrexR26-RFP* mice confirmed that ∼70% of LN LECs and BECs express the RFP reporter, indicating that the VE-cadherin-Cre transgene targets a major proportion of LTβR-expressing LN ECs.

Impact of EC-specific LTβR ablation on LN formation and structure

To ablate the LTβR on ECs, we crossed the *VE-cadherin-Cre* transgene onto the *Ltβr*$^{fl/fl}$ background (Wimmer et al., 2012). As shown in Fig. 3 a, *VE-cadherin-CrexLtβr*$^{fl/fl}$ mice failed to

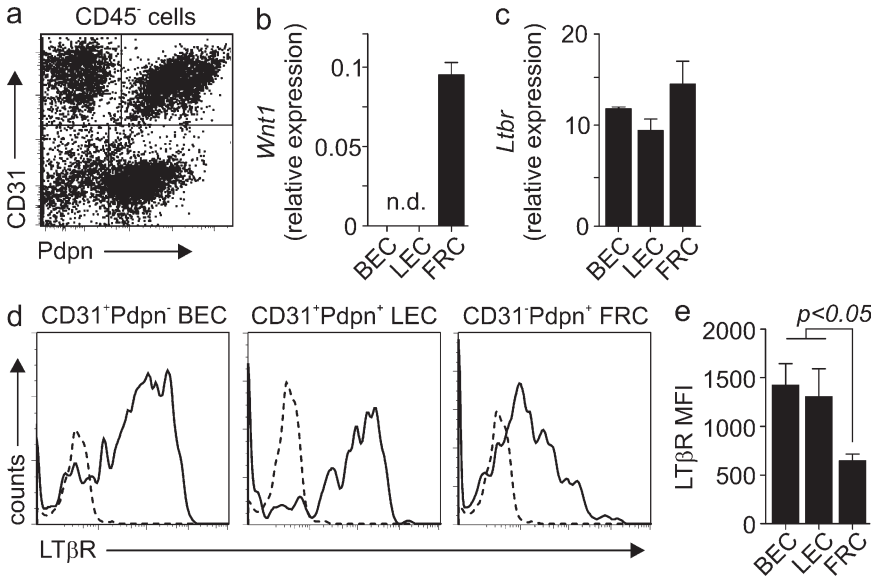

Figure 1. LTβR expression in LN endothelial and mesenchymal stromal cells. (a) CD45$^+$ hematopoietic cell–depleted cell suspensions from pooled peripheral LNs were stained with anti-CD31 and anti-Pdpn and analyzed by flow cytometry. FACS-sorted stromal subpopulations were analyzed for expression of (b) *Wnt1* and (c) *Ltbr* mRNA by real-time PCR (mean ± SEM from duplicate measurements; $n = 4$ independent samples analyzed in two independent experiments). (d) LTβR expression on different stromal cells as determined by flow cytometry (solid lines), dotted lines indicate isotype control staining of the respective population. (e) Mean fluorescence intensity (MFI) of LTβR expression on the indicated stromal cell populations (mean ± SEM; $n = 4$ mice, pooled from two independent experiments).

Published February 18, 2013

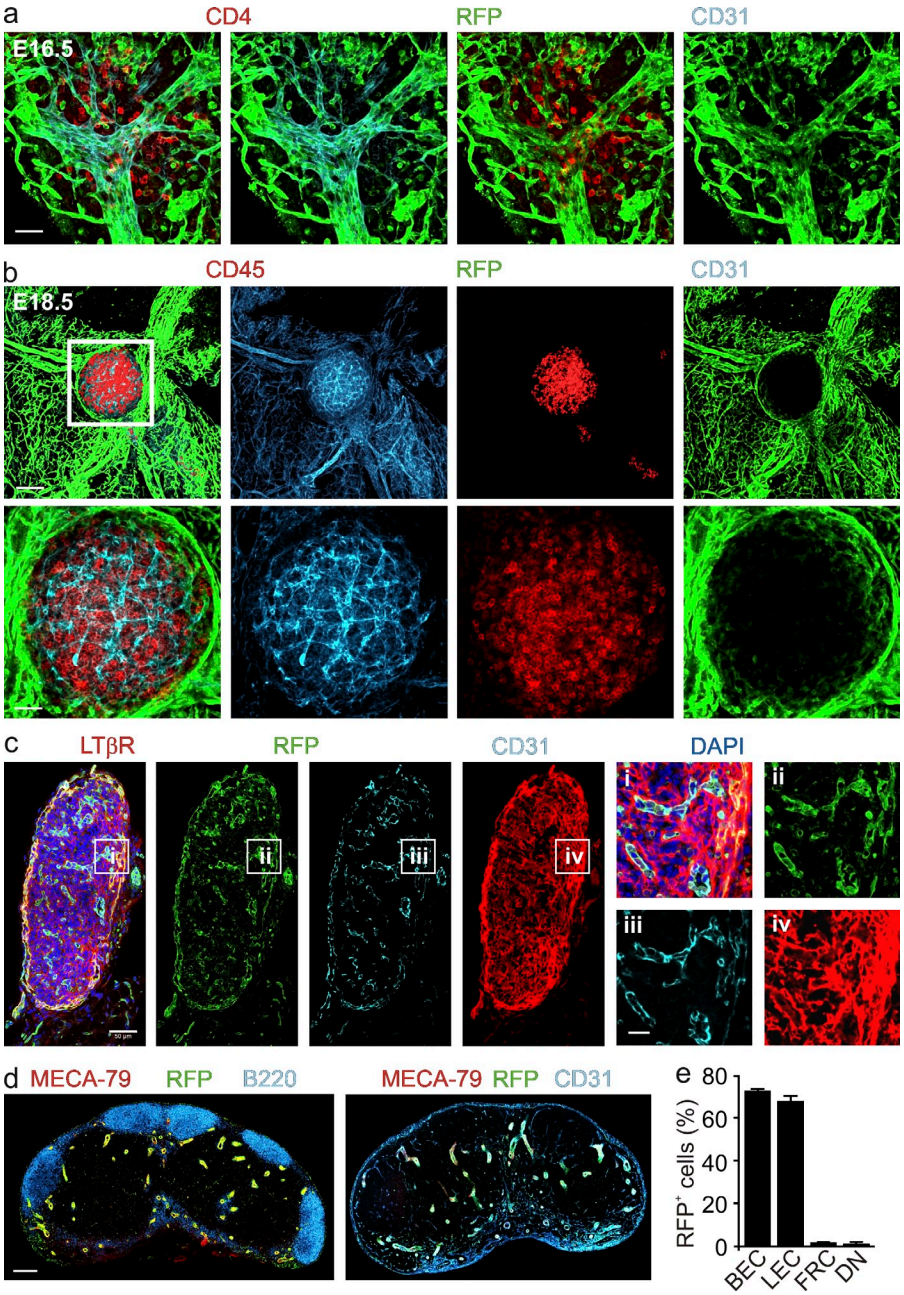

Figure 2. Targeting of LN endothelial cells in *VE-cadherin-Cre* mice. (a) Histological analysis of the inguinal LN anlage in *VE-Cadherin-CrexR26-RFP* embryos at E16.5. LN anlagen were stained in whole-mount with antibodies against RFP, CD31, and CD4. Bar, 20 µm. (b) Whole-mount histological analysis of the inguinal LN anlage in *VE-cadherin-CrexR26-RFP* embryos at E18.5 using the indicated antibodies. Top images show the overview of inguinal region with LN anlage embedded in the vasculature. Bar, 100 µm. Bottom shows magnification of boxed area in top image. Data show one representative analysis out of three. (c) LTβR expression in *VE-Cadherin-CrexR26-RFP* neonatal LNs. Sections were stained with antibodies against RFP, CD31, LTβR, and counterstained with DAPI. Boxed areas i–iv are annotated and shown in the right panels at higher magnification. Bars, 50 µm (20 µm for magnified insets). (d) Transgene expression in inguinal LNs of adult *VE-Cadherin-CrexR26-RFP* mice. Bar, 200 µm. Data show one representative analysis out of three. (e) Flow cytometric analysis of transgene expression (RFP) in $CD45^-$ LN stromal cells (mean ± SEM; $n = 6$ mice, pooled from two independent experiments).

develop 20–45% of their peripheral LNs. Injection of 1% Chicago Sky Blue solution one week before the analysis revealed that the loss of peripheral LNs in *VE-cadherin-CrexLtβr*$^{fl/fl}$ mice occurred in a random fashion with the failure to develop even rudimentary structures as shown in Fig. 3, b and c for the brachial or inguinal LN, respectively. Interestingly, formation of the mesenteric LN was not affected by the EC-specific LTβR deficiency (Fig. 3, a and d). Those peripheral LNs that had succeeded to develop in *VE-cadherin-CrexLtβr*$^{fl/fl}$ mice appeared smaller, as shown in Fig. 3 e for an inguinal LN. Optical projection tomographical (OPT) analysis of inguinal LNs confirmed the significant size differences between conditionally LTβR-deficient and control LNs (Fig. 3, f and g). As a consequence, the size of B cell follicles (Fig. 3 h), as well as overall cellularity (Fig. 3 i), were reduced. Furthermore, the OPT analysis revealed a profound structural deficiency in the vasculature, i.e., a severely impaired MECA-79$^+$ HEV network (Fig. 3 f). Quantification of HEV parameters revealed that the overall length of the MECA-79$^+$ vascular structures (Fig. 3 j) and the mean number of branching points (Fig. 3 k) were reduced by >60% and >70%, respectively. The exclusive impact of the conditional LTβR deficiency on ECs is shown by the preserved LTβR expression on FRCs, whereas both BECs and LECs in LNs of *VE-cadherin-CrexLtβr*$^{fl/fl}$ mice exhibited a significantly reduced LTβR expression (Fig. 3, l and m). In contrast to the profound effects

Published February 18, 2013

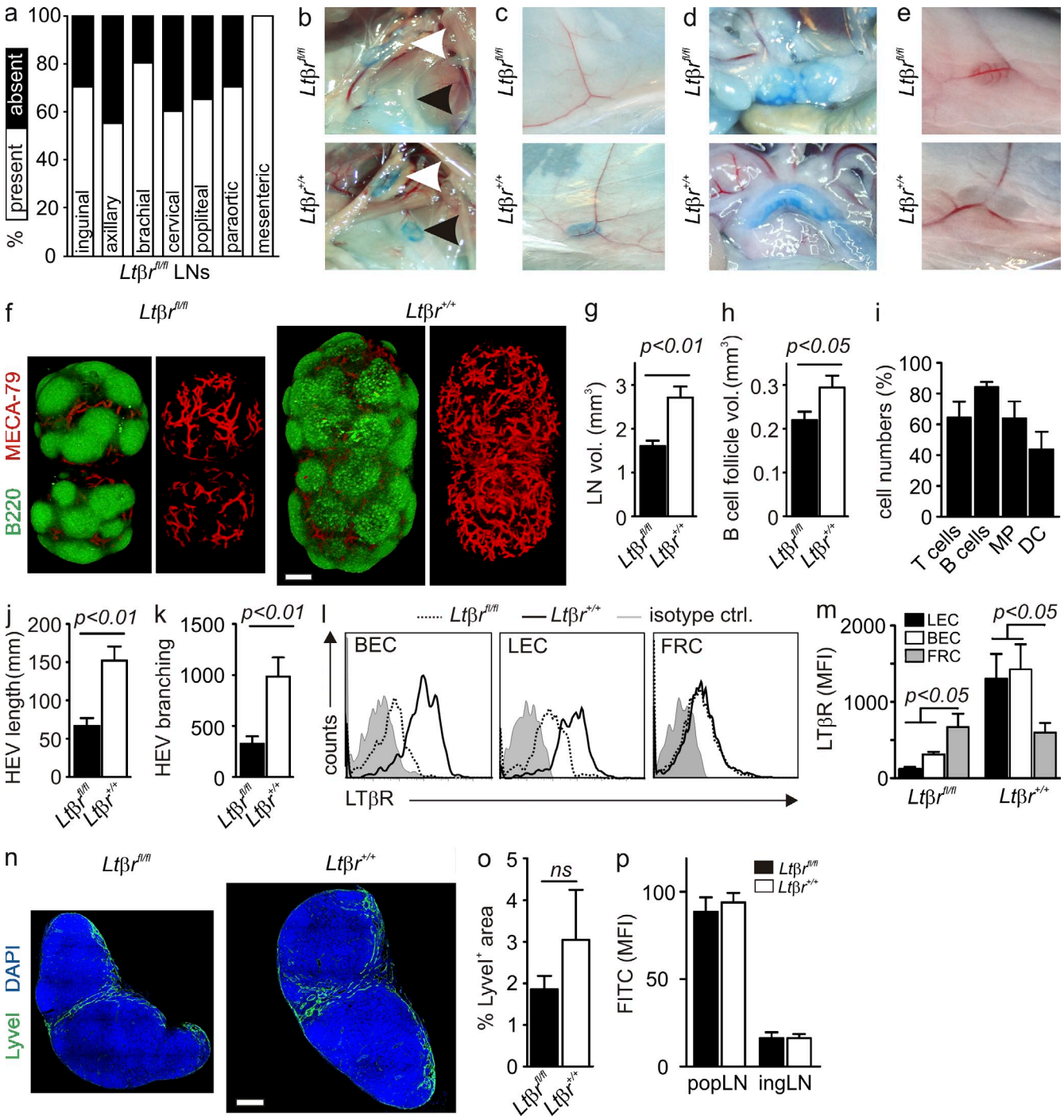

Figure 3. Ablation of LTβR signaling in ECs impacts peripheral LN development. (a) The presence of the indicated LNs was recorded in 4-wk-old *VE-cadherin-CrexLtβr*$^{fl/fl}$ mice and plotted as percent present/absent (n = 10 mice). Mice were injected with 1% Chicago sky blue 1 wk before the analysis. Microphotographs show presence or absence of (b) axillary (white arrow head) and brachial (black arrow head), (c) inguinal, or (d) mesenteric LNs in the indicated mouse strains. Representative microphotographs from one out of four mice per group. (e) Macroscopic appearance of developing inguinal LNs in *VE-cadherin-CrexLtβr*$^{fl/fl}$ mice (top image) and LTβR-proficient controls (bottom image). (f) Inguinal LNs from the indicated strains were analyzed by OPT for the presence of the HEV network (MECA-79$^+$) and B cell follicles (B220$^+$). Bar, 500 µm. Quantitative analysis based on OPT data for LN volume (g) and B cell follicle volume (h). (i) Flow cytometry–based quantification of LN cellularity. Values indicate relative cell numbers in *VE-cadherin-CrexLtβr*$^{fl/fl}$ mice compared with *Ltβr*$^{+/+}$ mice (mean ± SEM; n = 6 mice per group in 3 independent experiments). Quantitative analysis based on OPT data for (j) HEV network length and (k) HEV branching points (mean ± SEM; n = 6 mice per group pooled from three independent experiments). (l) Representative histograms showing flow cytometric analysis of LTβR expression on CD31$^+$Pdpn$^+$ LECs, CD31$^+$Pdpn$^-$ BECs, and CD31$^-$Pdpn$^+$ FRCs of *VE-cadherin-CrexLtβr*$^{fl/fl}$ and *Ltβr*$^{+/+}$ LNs. (m) Quantification of MFI for LTβR expression in respective populations (mean ± SEM from six mice per group, pooled from two independent

Published February 18, 2013

of the EC-specific LTβR ablation on the LN vasculature, the formation of intranodal lymphatic structures was less severely affected in the absence of EC-specific LTβR signaling (Fig. 3, n and o). Likewise, lymphatic skin drainage toward the popliteal LN and internodal lymph flow from the popliteal to the inguinal LN was not affected in *VE-cadherin-CrexLtβr$^{fl/fl}$* mice (Fig. 3 p). Collectively, these data suggest that the *VE-cadherin-Cre* transgene targets an early EC population that is LTβR dependent and is critical for LN development. Furthermore, in those adult LNs that succeeded in their development, likely due to the incomplete targeting of ECs in *VE-cadherin-Cre* mice (i.e., ∼70% of all LN BECs and LECs), a pronounced impact of direct LTβR signaling in ECs was evident.

Constitutive LTβR signaling in ECs is required for HEV formation and function

To further determine the consequences of EC-specific LTβR deficiency, we performed high-resolution confocal microscopy and assessed the phenotypical changes in HEV ECs. Despite the absence of LTβR signaling, ECs had maintained some MECA-79 expression (Fig. 4 a). Furthermore, the ERTR-7$^+$ FRC network surrounding the vascular structures was maintained (Fig. 4 a, arrowheads). However, the endothelium had lost its cuboidal shape and polarization, with decreased ICAM-1 staining on the luminal side (Fig. 4 a, arrow) resulting in a significantly reduced overall ICAM-1 expression (Fig. 4 b). Likewise, MECA-79$^+$ ECs in the conditionally LTβR-deficient mice had lost expression of CCL21 (Fig. 4 c, arrows, top left), whereas stromal cells surrounding the blood vessel still produced CCL21 as visualized in three-dimensional reconstructions of the paracortical stromal network (Fig. 4 c, right). Consistent with this finding, we found that the selective ablation of LTβR on ECs resulted in a reduction of *Ccl21* and *Ccl19* mRNA expression in total LN tissue (Fig. 4 d). Furthermore, expression of the HEV addressin *Glycam1* was almost completely lost in LNs of *VE-cadherin-CrexLtβr$^{fl/fl}$* mice, whereas the expression of the follicular dendritic cell marker *Mfge8* was not affected (Fig. 4 e). Collectively, the MECA-79$^+$ blood vessels in *VE-cadherin-CrexLtβr$^{fl/fl}$* mice had lost typical properties of HEVs.

To assess whether the structural and phenotypical alterations in MECA-79$^+$ blood vessels in *VE-cadherin-CrexLtβr$^{fl/fl}$* mice would impact on lymphocyte migration, we adoptively transferred dye-labeled lymphocytes and assessed their LN-homing behavior in *VE-cadherin-CrexLtβr$^{fl/fl}$* and control mice. As shown in Fig. 5 a, lymphocytes were still able to home to the LN parenchyma in *VE-cadherin-CrexLtβr$^{fl/fl}$* mice. However, flow cytometry–based quantification revealed that homing of both T and B cells was strongly affected by the EC-specific LTβR deficiency (Fig. 5 b). High-resolution microscopic analysis showed that adoptively transferred lymphocytes could be found within the HEVs of LTβR-competent mice (Fig. 5 c, bottom, arrows), whereas those lymphocytes that had successfully entered LNs of *VE-cadherin-CrexLtβr$^{fl/fl}$* mice were found exclusively in the LN parenchyma (Fig. 5 c, top, arrowheads). A recent study has shown that retention of lymphocytes in HEV pockets is an important regulatory step for lymphocyte trafficking (Mionnet et al., 2011). Indeed, in all LNs of LTβR-proficient mice, we found aggregates of CD4$^+$ T cells surrounded by the MECA-79$^+$ endothelium of HEVs (Fig. 5 d, bottom, arrows). However, this retention function was missing in the flat MECA-79$^+$ endothelium of LNs from *VE-cadherin-CrexLtβr$^{fl/fl}$* mice (Fig. 5 d, top). The CCR7 ligands CCL19 and CCL21 are important for the regulation of general T cell motility (Förster et al., 2008). Because we observed a general down-regulation of *Ccl19* and *Ccl21* in LNs of VE-cadherin-Crex*Ltβr$^{fl/fl}$* mice, we used intravital two-photon microscopy to determine whether general T cell motility would be affected by the EC-specific LTβR deficiency. As shown in Fig. 5 e, the specific LTβR defect in ECs and the resulting structural and functional alteration in the HEV network did not significantly impact on general T cell motility, neither in the T cell zone nor in the direct vicinity of MECA-79$^+$ vessels. Collectively, constitutive LTβR signaling in LN vascular ECs appears to be necessary for the differentiation of vascular ECs into the typical HEV EC and, hence, the appropriate formation of the HEV network.

The earliest steps in LN development involve the PROX1-dependent metamorphosis of venous ECs to lymphatic ECs at the anterior cardinal vein (Srinivasan et al., 2007). These early LECs form the lymph sac which serves as the primordial tissue for both the LN anlagen and the sprouting lymphatic system (Blum and Pabst, 2006). After these initial steps, mesenchymal LTo and hematopoietic LTi cells are recruited to the LN anlage and the subsequent developmental steps are dependent on the constitutive chemokine receptor ligands CXCL13, CCL19, and CCL21 (Luther et al., 2003). Furthermore, triggering of the CD127/IL-7Rα on LTi cells in concert with constitutive chemokine signals is critical for the formation of LNs and Peyer's patches. It has been suggested that LTβR signaling in mesenchymal LTo cells is the critical event that steers the cascading induction of constitutive chemokines and IL-7 (van de Pavert and Mebius, 2010). This particular view has been supported by the finding that the absence of lymphatic endothelium in PROX1-deficient mice did not block LN anlagen formation (Vondenhoff et al., 2009). The present study challenges the concept that there is only one dedicated LTβR-dependent stromal LTo cell

experiments). (n) Lymphatic sinus formation in inguinal LNs from the indicated mouse strains as determined by confocal microscopy using staining with anti-Lyvel. Bar, 200 µm. (o) Quantification of Lyvel$^+$ area in inguinal LNs from *VE-cadherin-CrexLtβr$^{fl/fl}$* and *Ltβr$^{+/+}$* mice (three sections per LN, values indicate mean ± SEM from six mice pooled from two independent experiments). (p) Accumulation of 40-kD FITC-dextran in draining LNs at 10 min after s.c. injection into the hind footpad. FITC fluorescence intensity on histological sections of popliteal and inguinal LN was quantified by confocal microscopy (three sections per LN, values indicate mean ± SEM from four mice pooled from two independent experiments).

Published February 18, 2013

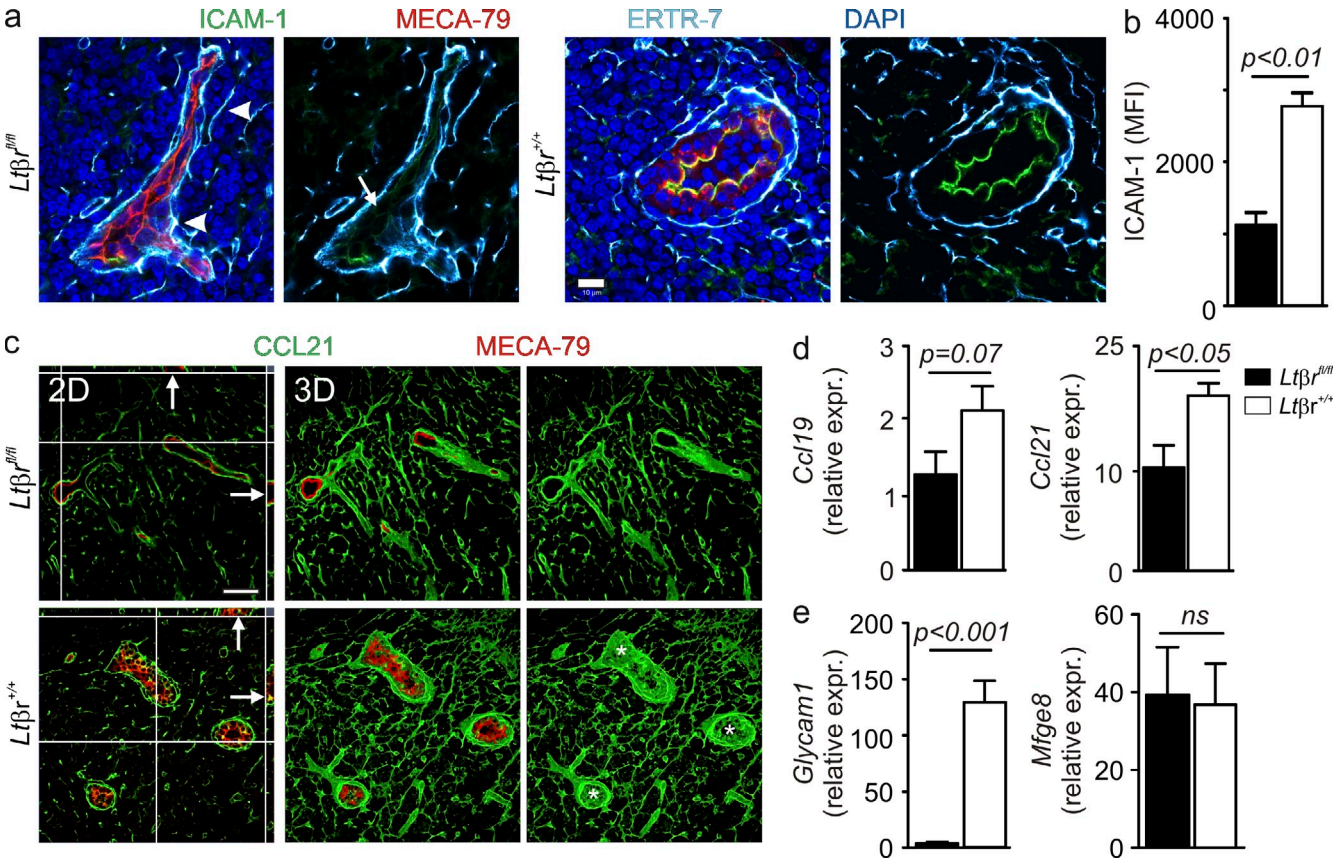

Figure 4. Impact of EC-specific LTβR deficiency on the MECA-79⁺ LN endothelium. (a) LN sections were stained with fluorescently labeled antibodies against ICAM-1, MECA-79, and ERTR-7 and analyzed by confocal microscopy. Bar, 10 µm. Arrowheads indicate presence of ERTR-7⁺ perivascular stroma, and arrow indicates decreased endothelial ICAM-1 expression. Data show one representative analysis out of five mice. (b) Flow cytometric determination of ICAM-1 expression (MFI) on CD31⁺Pdpn⁻ BECs in peripheral LNs from *VE-cadherin-CrexLtβr*$^{fl/fl}$ mice and *Ltβr*$^{+/+}$ mice (mean ± SEM from four mice per group, pooled from two independent experiments). (c) Confocal microscopic analysis of inguinal LN sections stained with fluorescently labeled antibodies against CCL21 and MECA-79, confocal sections (2D) with orthogonal display of the z-stack dimension at indicated x/y coordinates. Arrows indicate presence or absence of CCL21 expression on MECA-79⁺ vascular structures in z dimension. 3D reconstruction of z stacks are shown in right panel, stars indicate CCL21⁺MECA-79⁺ HEVs. Bar, 30 µm. Data show one representative analysis out of three. Quantitative RT-PCR analysis of *Ccl19* and *Ccl21* (d) and *Glycam1* and *Mfge8* (e) expression in inguinal LNs from *VE-cadherin-CrexLtβr*$^{fl/fl}$ and *Ltβr*$^{+/+}$ mice (mean ± SEM of duplicate measurements from four mice per group, pooled from two independent experiments).

population. We found that the ablation of LTβR expression in ECs in *VE-cadherin-CrexLtβr*$^{fl/fl}$ mice led to impaired LN development. Because the *VE-cadherin-Cre* transgene is active in ECs but not in mesenchymal stromal cells (Alva et al., 2006; this study), our study provides conclusive evidence that LTβR signaling in endothelial LTo cells is mandatory for LN formation. At this point, we can only speculate at which stage of LN development LTi cells interact with early endothelial LTo cells. It is possible that lymphotoxin-expressing LTi cells stimulate LTβR⁺ LECs in the early LN anlage to produce more CCL21, and thereby contribute to the CCR7 dependency of LN development (Luther et al., 2003). Moreover, the development of the intranodal blood vasculature may be dependent on LTβR signals provided to BECs. Insufficiently developed LN blood vessels may restrict LN formation because growing tissues are particularly vulnerable to impaired blood supply. Future studies of conditional and inducible LEC- versus BEC-specific ablation of the LTβR will reveal which of the two EC populations function as an endothelial LTo cell.

ECs and hematopoietic cells share the hemangioblast as a common precursor cell (Domigan and Iruela-Arispe, 2012) and therefore, some molecular traits are shared between the lineages. For example, VE-cadherin is involved in endothelial homotypic cell adhesion, a function that is critical for vascular development and function (Carmeliet et al., 1999). Consequently, the *VE-cadherin-Cre* transgene exhibits uniform expression in the endothelium of developing and quiescent vessels (Alva et al., 2006). However, a small proportion of hematopoietic cells express the *VE-cadherin-Cre* transgene (Alva et al., 2006). Among the different hematopoietic cell types, macrophages (Wimmer et al., 2012) express the LTβR and exhibit some functional changes after LTβR triggering. Nevertheless, because macrophage-specific ablation of the LTβR

Published February 18, 2013

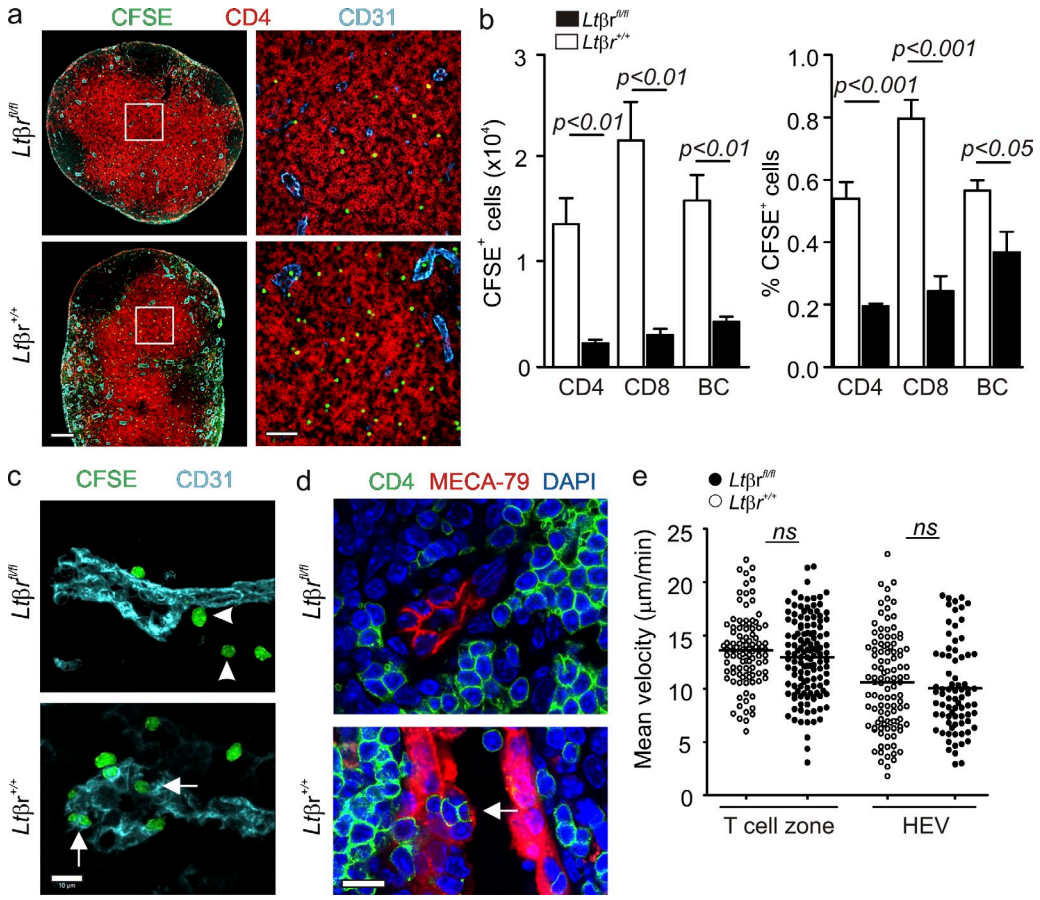

Figure 5. LTβR signaling in ECs is required for lymphocyte homeostasis. C57BL/6 splenocytes were labeled with CFSE and adoptively transferred into *VE-cadherin-CrexLtβr*$^{fl/fl}$ mice and *Ltβr*$^{+/+}$ mice. (a) Popliteal LN sections of indicated recipients were stained with fluorescently labeled antibodies against CD31, CD4, and CFSE and analyzed by confocal microscopy. Bar, 100 µm. (right) Higher magnification images of the boxed areas in the images on the left. Bar, 50 µm. Data show one representative analysis out of four. (b) Flow cytometric analysis of transferred cells (CFSE$^+$) lymphocytes in *VE-cadherin-CrexLtβr*$^{fl/fl}$ and *Ltβr*$^{+/+}$inguinal LNs. Left panel shows absolute numbers and right panel shows percentage of CFSE$^+$ cells in the respective population (mean ± SEM from 4 mice pooled from two independent experiments). (c) High-resolution analysis of CFSE$^+$ lymphocytes in (arrow) and around (arrowhead) CD31$^+$ vascular endothelia in LNs of *VE-cadherin-CrexLtβr*$^{fl/fl}$ and *Ltβr*$^{+/+}$ recipients. Bar, 10 µm. (d) Confocal microscopic analysis of intraendothelial pocket formation (arrow) in LNs of *VE-cadherin-CrexLtβr*$^{fl/fl}$ and *Ltβr*$^{+/+}$ recipients. Bar, 10 µm. (e) Lymphocyte motility in the T cell zone and around HEV in popliteal LNs of *VE-cadherin-CrexLtβr*$^{fl/fl}$ and *Ltβr*$^{+/+}$ mice as determined by intravital two-photon microscopy. Values represent single tracks pooled from two independent experiments (n = 4 mice per group, mean indicated by horizontal bar).

did not affect LN formation (Wimmer et al., 2012), we conclude that the defect in LN development in *VE-cadherin-CrexLtβr*$^{fl/fl}$ mice is a direct result of LTβR deficiency in ECs.

Concluding remarks

The characterization of the developmental pathways of LN organogenesis is most helpful for the understanding of the primary functions of these immune compartments in the adult, namely concentration of pathogens and immune cells to secure swift activation of innate and adaptive immunity (Junt et al., 2008). During immune activation, LNs undergo profound morphological changes to optimally accommodate or restore particular interaction compartments. For example, the LTβR-dependent interaction of adult LTi cells with T cell zone FRCs is critical for the restoration of immunocompetence after viral infection (Scandella et al., 2008). Furthermore, B cell–derived lymphotoxin significantly contributes to the remodeling and adaptation of the HEV network during the acute phase of a noncytopathic viral infection (Kumar et al., 2010). It has also been suggested that restructuring of the vascular LN microenvironment can be mediated by dendritic cells (Chyou et al., 2011). Likewise, the LTβR-dependent, homeostatic control of the adult LN HEV network (Browning et al., 2005) may be a result of multicellular processes (Chyou et al., 2008). The results of this study indicate that direct triggering of the LTβR on vascular ECs is important for the development of the cuboidal HEV appearance and the acquisition of lymphocyte traffic–regulating properties such as polarized ICAM1 expression, production of CCL21, and formation of pouches for lymphocyte retention. These findings bear interesting implications for the formation of tertiary lymphoid tissues in the course of infections and autoimmune diseases:

Published February 18, 2013

chronically activated, lymphotoxin-expressing lymphocytes may directly induce the differentiation of ECs into the HEV phenotype, hence recapitulating the generation of the vascular LN microenvironment for optimal lymphocyte trafficking (Hayasaka et al., 2010). Further molecular dissection of this pathway may help to identify targets that attenuate the formation of tertiary lymphoid tissues at sites of chronic inflammation.

MATERIALS AND METHODS

Mice. B6.Cg-Tg(Cdh5-cre)7Mlia/J (*VE-Cadherin-Cre*; Alva et al., 2006) and B6.129X1-Gt(ROSA)26Sor^{tm1Hjf} (*R26-RFP*) mice were purchased from The Jackson Laboratory. *Ltbr*$^{fl/fl}$ mice were described previously (Wimmer et al., 2012). C57BL/6 mice were obtained from Charles River. All animals were kept under conventional conditions in individually ventilated cages. Experiments were performed in accordance with federal and cantonal guidelines (Tierschutzgesetz) under the permission numbers SG11/05 and SG11/04 granted by the Veterinary Office of the Canton of St. Gallen.

CFSE-labeling and adoptive transfer of cells. Single-cell suspensions from spleens of C57BL/6 mice were subjected to hypotonic red blood cell lysis and stained with CFSE (Molecular Probes). A maximum concentration of 2.5×10^7 cells/ml were incubated in 5 µM CFSE in PBS for 10 min at 37°C. Cells were washed twice with ice-cold balanced salt solution (BSS) and resuspended in BSS. *VE-Cadherin-Crex Ltbr*$^{fl/fl}$ or control mice were injected intravenously with 10^7 C57BL/6 splenocytes in 200 µl BSS. Homing of transferred cells was analyzed 2 h after transfer by flow cytometry and histology.

Preparation of stromal cells. LNs were dissected into small pieces and transferred into a 24-well dish filled with RPMI 1640 medium containing 2% FCS, 20 mM Hepes (all from Lonza), 1 mg/ml Collagenase Type IV (Sigma-Aldrich), and 25 µg/ml DNaseI (AppliChem). Dissociated LNs were incubated at 37°C for 30 min. After enzymatic digestion, cell suspensions were washed with PBS containing 0.5% FCS and 10 mM EDTA (MACS buffer). To further enrich the stromal cell fraction, hematopoietic cells were depleted by incubating the cell suspension with MACS anti-CD45 Microbeads and passing over a MACS LS column (Miltenyi Biotec).

Flow cytometry and cell sorting. Single-cell suspensions were incubated for 20 min at 4°C in PBS containing 1% FCS and 10 mM EDTA with the following fluorescently labeled antibodies: anti-CD45, anti-gp38/podoplanin (BD), anti-CD31, anti-LTβR (eBioscience), anti-CD4, anti-CD8, anti-CD11c, anti-CD11b, and anti-F4/80 (BioLegend). Cells were acquired with a FACS Canto (BD) and analyzed using FlowJo software (Tree Star). Cell sorting was performed using a FACS Aria cell sorter (BD).

Quantitative real time PCR. Total cellular RNA was extracted from homogenized tissues and sorted cells using TRIzol reagent (Invitrogen) following the manufacturer's protocol. cDNA was prepared using cDNA archive kit (Applied Biosystems), and quantitative RT-PCR was performed using the Light Cycler-FastStart DNA Master SYBR Green I kit (Roche) on a LightCycler machine (Roche). Expression levels were measured using the following primers: *Wnt1*; *Mfge8*; QT00098917; *Glycam1*; QT00141526 (QuantiTect primer assay; QT00103985; QIAGEN); *Ccl19*, forward 5′-CTGCCTCAGATTATCTGCCAT-3′, reverse 5′-AGGTAGCGGAAGGCTTTCAC-3′; *Ccl21*, forward 5′-AAGGCAGTGATGGAGGGG-3′, reverse 5′-CGGGGTAAGAACAGGATTG-3′; tata-box binding protein (tbp), forward 5′-CCTTCACCAATGACTCCTATGAC-3′, reverse 5′-CAAGTTTACAGCCAAGATTCAC-3′.

Immunohistochemistry. LNs were fixed over night in freshly prepared 4% paraformaldehyde (Merck) at 4°C under agitation. Fixed LNs were embedded in 4% low melting agarose (Invitrogen) in PBS and sectioned with a vibratome (VT-1200; Leica). 20–30-µm-thick sections were blocked in PBS containing 10% FCS, 1 mg/ml anti-FcRγ (BD) and 0.1% Triton X-100 (Sigma-Aldrich). Sections were incubated over night at 4°C with the following antibodies: anti-RFP, anti-CCL21 (Abcam), anti-gp38/podoplanin, anti-CD45, anti-B220, conjugated anti-CD31, anti-LyveI (eBioscience), anti-CD4, anti–ICAM-1 (BioLegend), and anti MECA-79. Unconjugated antibodies were detected with the following secondary antibodies: Dylight649-conjugated anti–rat-IgG, Alexa Fluor 488–conjugated anti–rabbit-IgG, Dylight549-conjugated anti–Syrian hamster-IgG, and Dylight549-conjugated Streptavidin (all purchased from Jackson ImmunoResearch Laboratories). Fluorescence signal of LTβR staining was amplified by using a tyramide-amplification kit (Molecular Probes) according to the manufacturer's protocol. Microscopic analysis was performed using a confocal microscope (LSM-710; Carl Zeiss) and images were processed with ZEN 2010 software (Carl Zeiss). For tracing of lymphatic flow, mice were injected with 50 µg of 40-kD FITC-dextran into the hind footpad. 10 min after injection, mice were sacrificed and draining LNs were carefully excised under the stereomicroscope, fixed, and cut with a vibratome (VT-1200; Leica). FITC fluorescence per LN section was quantified using the LSM-710 confocal microscope.

OPT. Mice received an intravenous injection of fluorescently labeled MECA-79 (12–15 µg) to label the HEV network. After 15 min, mice were sacrificed, LNs were carefully excised, and surrounding tissue was removed under a stereomicroscope. Sample preparation and OPT were performed as previously described (Kumar et al., 2010).

Intravital microscopy. Purified C57BL/6 T cells were fluorescently labeled with 2.5 µM chloromethyl-benzoyl amino-tetramethylrhodamine or CFSE for 15 min at 37°C. After washing, labeled T cells were injected intravenously into sex-matched mice, which were anesthetized and surgically prepared to expose the right popliteal LN. Immediately after injection, two-photon microscopy was performed as previously described (Soriano et al., 2011).

Statistical analysis. Two-photon microscopy and OPT data were analyzed with Volocity (Perkin Elmer) and Imaris (Bitplane). All statistical analyses were performed with Prism 5.0 (GraphPad Software Inc.). Data were analyzed with the nonpaired Student's *t* test. A p-value of <0.05 was considered significant.

We would like to thank Rita DeGiuli for technical support.

This study received financial support from the Swiss National Science Foundation (Sinergia 125447/1 to J.V. Stein and B. Ludewig and 130823/1 to B. Ludewig).

The authors declare no potential conflict of interest.

Author contributions: B. Ludewig designed the study and wrote the paper; L. Onder performed research and wrote the paper; E. Scandella, J.V. Stein, and T. Hehlgans analyzed data; R. Danuser, S. Firner, and Qian Chai performed research.

Submitted: 5 July 2012
Accepted: 18 January 2013

REFERENCES

Alva, J.A., A.C. Zovein, A. Monvoisin, T. Murphy, A. Salazar, N.L. Harvey, P. Carmeliet, and M.L. Iruela-Arispe. 2006. VE-Cadherin-Cre-recombinase transgenic mouse: a tool for lineage analysis and gene deletion in endothelial cells. *Dev. Dyn.* 235:759–767. http://dx.doi.org/10.1002/dvdy.20643

Bénézech, C., A. White, E. Mader, K. Serre, S. Parnell, K. Pfeffer, C.F. Ware, G. Anderson, and J.H. Caamaño. 2010. Ontogeny of stromal organizer cells during lymph node development. *J. Immunol.* 184:4521–4530. http://dx.doi.org/10.4049/jimmunol.0903113

Blum, K.S., and R. Pabst. 2006. Keystones in lymph node development. *J. Anat.* 209:585–595. http://dx.doi.org/10.1111/j.1469-7580.2006.00650.x

Braun, A., T. Worbs, G.L. Moschovakis, S. Halle, K. Hoffmann, J. Bölter, A. Münk, and R. Förster. 2011. Afferent lymph-derived T cells and DCs use different chemokine receptor CCR7-dependent routes for entry into the lymph node and intranodal migration. *Nat. Immunol.* 12:879–887. http://dx.doi.org/10.1038/ni.2085

Browning, J.L., and L.E. French. 2002. Visualization of lymphotoxin-beta and lymphotoxin-beta receptor expression in mouse embryos. *J. Immunol.* 168:5079–5087.

Browning, J.L., N. Allaire, A. Ngam-Ek, E. Notidis, J. Hunt, S. Perrin, and R.A. Fava. 2005. Lymphotoxin-beta receptor signaling is required for the homeostatic control of HEV differentiation and function. *Immunity.* 23:539–550. http://dx.doi.org/10.1016/j.immuni.2005.10.002

Carmeliet, P., M.G. Lampugnani, L. Moons, F. Breviario, V. Compernolle, F. Bono, G. Balconi, R. Spagnuolo, B. Oosthuyse, M. Dewerchin, et al. 1999. Targeted deficiency or cytosolic truncation of the VE-cadherin gene in mice impairs VEGF-mediated endothelial survival and angiogenesis. *Cell.* 98:147–157. http://dx.doi.org/10.1016/S0092-8674(00)81010-7

Chyou, S., E.H. Ekland, A.C. Carpenter, T.C. Tzeng, S. Tian, M. Michaud, J.A. Madri, and T.T. Lu. 2008. Fibroblast-type reticular stromal cells regulate the lymph node vasculature. *J. Immunol.* 181:3887–3896.

Chyou, S., F. Benahmed, J. Chen, V. Kumar, S. Tian, M. Lipp, and T.T. Lu. 2011. Coordinated regulation of lymph node vascular-stromal growth first by CD11c+ cells and then by T and B cells. *J. Immunol.* 187:5558–5567. http://dx.doi.org/10.4049/jimmunol.1101724

Domigan, C.K., and M.L. Iruela-Arispe. 2012. Recent advances in vascular development. *Curr. Opin. Hematol.* 19:176–183. http://dx.doi.org/10.1097/MOH.0b013e3283523e90

Förster, R., A.C. Davalos-Misslitz, and A. Rot. 2008. CCR7 and its ligands: balancing immunity and tolerance. *Nat. Rev. Immunol.* 8:362–371. http://dx.doi.org/10.1038/nri2297

Fütterer, A., K. Mink, A. Luz, M.H. Kosco-Vilbois, and K. Pfeffer. 1998. The lymphotoxin beta receptor controls organogenesis and affinity maturation in peripheral lymphoid tissues. *Immunity.* 9:59–70. http://dx.doi.org/10.1016/S1074-7613(00)80588-9

Grigorova, I.L., M. Panteleev, and J.G. Cyster. 2010. Lymph node cortical sinus organization and relationship to lymphocyte egress dynamics and antigen exposure. *Proc. Natl. Acad. Sci. USA.* 107:20447–20452. http://dx.doi.org/10.1073/pnas.1009968107

Hayasaka, H., K. Taniguchi, S. Fukai, and M. Miyasaka. 2010. Neogenesis and development of the high endothelial venules that mediate lymphocyte trafficking. *Cancer Sci.* 101:2302–2308. http://dx.doi.org/10.1111/j.1349-7006.2010.01687.x

Junt, T., E. Scandella, and B. Ludewig. 2008. Form follows function: lymphoid tissue microarchitecture in antimicrobial immune defence. *Nat. Rev. Immunol.* 8:764–775. http://dx.doi.org/10.1038/nri2414

Kumar, V., E. Scandella, R. Danuser, L. Onder, M. Nitschké, Y. Fukui, C. Halin, B. Ludewig, and J.V. Stein. 2010. Global lymphoid tissue remodeling during a viral infection is orchestrated by a B cell-lymphotoxin-dependent pathway. *Blood.* 115:4725–4733. http://dx.doi.org/10.1182/blood-2009-10-250118

Luther, S.A., K.M. Ansel, and J.G. Cyster. 2003. Overlapping roles of CXCL13, interleukin 7 receptor alpha, and CCR7 ligands in lymph node development. *J. Exp. Med.* 197:1191–1198. http://dx.doi.org/10.1084/jem.20021294

Malhotra, D., A.L. Fletcher, J. Astarita, V. Lukacs-Kornek, P. Tayalia, S.F. Gonzalez, K.G. Elpek, S.K. Chang, K. Knoblich, M.E. Hemler, et al; Immunological Genome Project Consortium. 2012. Transcriptional profiling of stroma from inflamed and resting lymph nodes defines immunological hallmarks. *Nat. Immunol.* 13:499–510. http://dx.doi.org/10.1038/ni.2262

Mionnet, C., S.L. Sanos, I. Mondor, A. Jorquera, J.P. Laugier, R.N. Germain, and M. Bajénoff. 2011. High endothelial venules as traffic control points maintaining lymphocyte population homeostasis in lymph nodes. *Blood.* 118:6115–6122. http://dx.doi.org/10.1182/blood-2011-07-367409

Moussion, C., and J.P. Girard. 2011. Dendritic cells control lymphocyte entry to lymph nodes through high endothelial venules. *Nature.* 479:542–546. http://dx.doi.org/10.1038/nature10540

Oliver, G., and R.S. Srinivasan. 2008. Lymphatic vasculature development: current concepts. *Ann. N. Y. Acad. Sci.* 1131:75–81. http://dx.doi.org/10.1196/annals.1413.006

Scandella, E., B. Bolinger, E. Lattmann, S. Miller, S. Favre, D.R. Littman, D. Finke, S.A. Luther, T. Junt, and B. Ludewig. 2008. Restoration of lymphoid organ integrity through the interaction of lymphoid tissue-inducer cells with stroma of the T cell zone. *Nat. Immunol.* 9:667–675. http://dx.doi.org/10.1038/ni.1605

Soriano, S.F., M. Hons, K. Schumann, V. Kumar, T.J. Dennier, R. Lyck, M. Sixt, and J.V. Stein. 2011. In vivo analysis of uropod function during physiological T cell trafficking. *J. Immunol.* 187:2356–2364. http://dx.doi.org/10.4049/jimmunol.1100935

Srinivasan, R.S., M.E. Dillard, O.V. Lagutin, F.J. Lin, S. Tsai, M.J. Tsai, I.M. Samokhvalov, and G. Oliver. 2007. Lineage tracing demonstrates the venous origin of the mammalian lymphatic vasculature. *Genes Dev.* 21:2422–2432. http://dx.doi.org/10.1101/gad.1588407

Tohya, K., E. Umemoto, and M. Miyasaka. 2010. Microanatomy of lymphocyte-endothelial interactions at the high endothelial venules of lymph nodes. *Histol. Histopathol.* 25:781–794.

Turley, S.J., A.L. Fletcher, and K.G. Elpek. 2010. The stromal and haematopoietic antigen-presenting cells that reside in secondary lymphoid organs. *Nat. Rev. Immunol.* 10:813–825. http://dx.doi.org/10.1038/nri2886

van de Pavert, S.A., and R.E. Mebius. 2010. New insights into the development of lymphoid tissues. *Nat. Rev. Immunol.* 10:664–674. http://dx.doi.org/10.1038/nri2832

Vondenhoff, M.F., S.A. van de Pavert, M.E. Dillard, M. Greuter, G. Goverse, G. Oliver, and R.E. Mebius. 2009. Lymph sacs are not required for the initiation of lymph node formation. *Development.* 136:29–34. http://dx.doi.org/10.1242/dev.028456

Wimmer, N., B. Huber, N. Barabas, J. Röhrl, K. Pfeffer, and T. Hehlgans. 2012. Lymphotoxin β receptor activation on macrophages induces cross-tolerance to TLR4 and TLR9 ligands. *J. Immunol.* 188:3426–3433. http://dx.doi.org/10.4049/jimmunol.1103324